New generation of the reference interaction site model self-consistent field method: Introduction of spatial electron density distribution to the solvation theory

Daisuke Yokogawa, Hirofumi Sato,[a] and Shigeyoshi Sakaki
Department of Molecular Engineering, Graduate School of Engineering, Kyoto University, Nishikyo-ku, Kyoto 615-8510, Japan

(Received 8 March 2007; accepted 27 April 2007; published online 25 June 2007)

The authors propose the new generation of the reference interaction site model self-consistent field (RISM-SCF) method for the solvation effect on the electronic structure of a solute molecule, in which the procedure proposed by Gill *et al.* [J. Chem. Phys. **96**, 7178 (1992)] is adopted. Main improvements are the introduction of spatial electron density distribution and the removal of the grid dependency that is inherent in the original RISM-SCF. The procedure also provides very stable determination of the effective charges even if a buried atom exists in the target molecule and eventually extends the applicability of the RISM-SCF. To demonstrate the superiority of our method, sample calculations for H_2O, C_2H_5OH, and HLi in aqueous solution are presented. © *2007 American Institute of Physics*. [DOI: 10.1063/1.2742380]

I. INTRODUCTION

Quantum molecular orbital calculation (MO calculation) with solvation effect is a fundamental tool in the theoretical study of chemical physics in solution. Many solvation theories have been proposed for investigation of chemical process in solvation phase.

In dielectric continuum model, such as polarizable continuum model (PCM),[1] solvent molecules are replaced by macroscopic media with dielectric constant. The electronic structure is solved in vacuum cavity surrounded by the dielectric continuum. In quantum mechanics/molecular mechanics (QM/MM) simulations, the neighboring solvent molecules around a solute molecule are treated explicitly. The electronic structure and solvation structure are calculated by averaging over various solvent configurations. Although these methods have been widely employed, the former oversimplifies microscopic characters of solvent and the latter requires large computational cost for the generation of the solvent configurations. Reference interaction site model self-consistent field[2,3] (RISM-SCF) is another method, in which solvation structure is provided by an integral equation theories based on statistical mechanics of molecular liquids (RISM).[4,5] RISM-SCF offers not only various macroscopic thermodynamic quantities but also microscopic properties such as radial distribution functions (RDFs) with reasonable computational cost. RISM-SCF has been successfully applied to understand the interplay between the electronic structure and solvation structure.[6]

In the treatment of solvation effect, Coulomb interaction between solute and solvent molecules is primarily important factor in most cases. A common representation for the interaction is the sum of pairwise interaction between point charges assigned on each atom. The most popular method to set the charges is the least-squares fitting (LSF) procedure, in which the effective charges are determined so that the electrostatic potential (ESP) derived from MO calculation can be reproduced at a set of grid points. Although the LSF procedure, which is employed for the original RISM-SCF,[2] is very simple, several weak points have been pointed out so far. For example, the atomic charges depend on the choice of the set of grid points. When buried atoms exist in the molecule, the evaluation of the atomic charges is often ill behaved. Besides, the representation of point charges neglects spread of electron distribution.

To obtain more realistic Coulomb interaction, another strategy has been used in quantum chemical study, especially in the field of density functional theory. In this strategy, the auxiliary basis sets (ABSs) on each atom are prepared to divide electron density into the components assigned on each atom. Gill *et al.* proposed a procedure to determine ABSs which reproduce the ESP provided by MO calculation (GJPT procedure).[7] The great advantage of GJPT procedure is that it treats directly spatial electron density distribution (SEDD) and does not require the set of grid points; it is free from these artificial parameters. As described later, GJPT procedure is very stable to determine the charges even if a buried site is involved in the solute molecule.

In this paper, we propose the new-generation RISM-SCF, in which GJPT procedure is employed. The present method, RISM-SCF explicitly including SEDD (RISM-SCF-SEDD), is much more robust in the connection between RISM and MO calculation than the original version of RISM-SCF and significantly expands the versatility of the RISM-SCF family. In Sec. II, the RISM-SCF-SEDD formalism and the relation between GJPT and LSF procedures are presented. In Sec. III, the computational details of this work are described. The results of H_2O, C_2H_5OH, and HLi evaluated by RISM-SCF-SEDD are shown in Sec. IV.

[a]Electronic mail: hirofumi@moleng.kyoto-u.ac.jp

II. METHOD

A. The formalism of RISM-SCF-SEDD

In GJPT procedure, model electron density $\tilde{\rho}$ is determined so that the ESP calculated by MO calculation can be reproduced, under the constraint of conservation of total number of electron. Gill *et al.* showed that $\tilde{\rho}$ can be obtained by minimizing the following quantity:

$$\Gamma = -2\pi \int\int (\rho(\mathbf{r}_1) - \tilde{\rho}(\mathbf{r}_1))|\mathbf{r}_1 - \mathbf{r}_2|(\rho(\mathbf{r}_2) - \tilde{\rho}(\mathbf{r}_2))d\mathbf{r}_1 d\mathbf{r}_2 + 2\lambda\left[N_e - \int \tilde{\rho}(\mathbf{r})d\mathbf{r}\right], \quad (1)$$

where N_e is the number of electrons and ρ is the electron density derived from MO calculation. $\tilde{\rho}(\mathbf{r})$ is represented by the set of ABSs $f_i(\mathbf{r})$ centered on each solute site,

$$\tilde{\rho}(\mathbf{r}) = \sum_i^{N_{\mathrm{ABS}}} d_i f_i(\mathbf{r}), \quad (2)$$

where N_{ABS} is the number of ABSs.[8] The expansion coefficients d in Eq. (2) can be determined by the following equations:

$$\mathbf{d} = \mathbf{X}^{-1}\,\mathrm{tr}(\mathbf{PY}) - \lambda\mathbf{X}^{-1}\mathbf{Z}, \quad (3)$$

$$\lambda = \frac{\mathbf{Z}^t\mathbf{X}^{-1}\,\mathrm{tr}(\mathbf{PY}) - N_e}{\mathbf{Z}^t\mathbf{X}^{-1}\mathbf{Z}}, \quad (4)$$

using the density matrix $\{P_{\mu\nu}\}(=\Sigma_i n_i C_{\mu i} C_{\nu i}^*)$ calculated from MO coefficients $\{C_{\mu i}\}$ and occupation number n_i. The components of the matrix $\mathbf{X}$, $\mathbf{Y}$, and $\mathbf{Z}$ are defined, as follows:

$$X_{ij} = \int\int f_i(\mathbf{r}_1)|\mathbf{r}_1 - \mathbf{r}_2|f_j(\mathbf{r}_2)d\mathbf{r}_1 d\mathbf{r}_2, \quad (5)$$

$$Y_{\mu\nu,i} = \int\int \phi_\mu(\mathbf{r}_1)\phi_\nu(\mathbf{r}_1)|\mathbf{r}_1 - \mathbf{r}_2|f_j(\mathbf{r}_2)d\mathbf{r}_1 d\mathbf{r}_2, \quad (6)$$

$$Z_i = \int f_i(\mathbf{r})d\mathbf{r}, \quad (7)$$

where ϕ is the basis function employed in MO calculation.

The effective electrostatic interaction between f_i and solvent is then given by[2]

$$V_i = n^V \sum_\gamma q_\gamma \int\int \frac{f_i(\mathbf{r}' - \mathbf{r}_\alpha)}{|\mathbf{r} - \mathbf{r}'|} h_{\alpha\gamma}(|\mathbf{r} - \mathbf{r}_\alpha|)d\mathbf{r}d\mathbf{r}' \quad (i \in \alpha), \quad (8)$$

where $h_{\alpha\gamma}$ is total correlation function between solute site α and solvent site γ. q_γ is partial charge of solvent site γ, n^V is the number density of solvent, and $\mathbf{r}_\alpha$ is the coordinate of solute site α. By employing the standard procedure in RISM-SCF,[2,3] the solvated Fock matrix is given by

$$\mathbf{H}^{\mathrm{solv}} = \mathbf{H}^{\mathrm{gas}} - \mathbf{V}\mathbf{X}^{-1}\mathbf{Y} + \frac{\mathbf{V}\mathbf{X}^{-1}\mathbf{Z}}{\mathbf{Z}^t\mathbf{X}^{-1}\mathbf{Z}}[\mathbf{Z}^t\mathbf{X}^{-1}\mathbf{Y} - \mathbf{S}], \quad (9)$$

where $\mathbf{H}^{\mathrm{gas}}$ is the Fock matrix in gas phase and $\mathbf{S}$ is overlap matrix.

B. The relationship between GJPT and LSF procedures

In this section, we would like to make a brief comment on the relationship between GJPT and LSF procedures. In the standard LSF procedure, atomic population $\mathbf{q}$ is determined by the following equation;[2]

$$\mathbf{q} = \mathbf{A}^{-1}\,\mathrm{tr}(\mathbf{PB}) - \lambda\mathbf{A}^{-1}\mathbf{1}, \quad (10)$$

$$\lambda = \frac{\mathbf{1}^t\mathbf{A}^{-1}\,\mathrm{tr}(\mathbf{PB}) - N_e}{\mathbf{1}^t\mathbf{A}^{-1}\mathbf{1}}. \quad (11)$$

The components of A and B are defined as follows:

$$A_{\alpha\beta} = \sum_{k=1}^{l} \frac{1}{|\mathbf{r}_k - \mathbf{r}_\alpha||\mathbf{r}_k - \mathbf{r}_\beta|}, \quad (12)$$

$$B_{\mu\nu\alpha} = \sum_{k=1}^{l} \int \frac{\phi_\mu(\mathbf{r}_1)\phi_\nu(\mathbf{r}_1)}{|\mathbf{r}_k - \mathbf{r}_\alpha||\mathbf{r}_k - \mathbf{r}_1|}d\mathbf{r}_1, \quad (13)$$

where $\mathbf{r}_k$ are the coordinates of grid point and $\mathbf{r}_\alpha$ are those of solute site.

Comparing Eqs. (3) and (10), the stability of the charge determination depends on the character of $\mathbf{X}^{-1}$ and $\mathbf{A}^{-1}$. In the case of LSF procedure, $\mathbf{A}$ is calculated from the grid set around the solute molecule. Since grid point $\mathbf{r}_k$ is far from $\mathbf{r}_\alpha$ (or $\mathbf{r}_\beta$) in most cases ($|\mathbf{r}_k - \mathbf{r}_M| \gg |\mathbf{r}_{\alpha/\beta} - \mathbf{r}_M|$), Eq. (12) is

$$A_{\alpha\beta} = \sum_k^l \frac{1}{|(\mathbf{r}_k - \mathbf{r}_M) - (\mathbf{r}_\alpha - \mathbf{r}_M)||(\mathbf{r}_k - \mathbf{r}_M) - (\mathbf{r}_\beta - \mathbf{r}_M)|} \sim \sum_k \frac{1}{|\mathbf{r}_k - \mathbf{r}_M|^2} = \mathrm{const}, \quad (14)$$

where $\mathbf{r}_M$ is the arbitrary point in the molecule (for example, the center of mass). Thus all the components of $\mathbf{A}$ tend to be very similar to each other and the behavior of inverse of such matrix sometimes becomes unstable.[9] On the other hand, the components of Eq. (5) are much characterized only by the center of ABSs, f_i and f_j. Therefore, the components of $\mathbf{X}$ are very different from each other and $\mathbf{X}^{-1}$ is robustly given compared to $\mathbf{A}^{-1}$. The advantage of GJPT procedure relative to LSF procedure is mainly from this different character.

III. COMPUTATIONAL DETAILS

In the present study, normal Gaussian functions are employed for ABSs,

$$f_i(\mathbf{r}) = C_i \exp(-\alpha_i r^2), \quad (15)$$

where C_i is an appropriate coefficient.[10] Equation (8) is simplified as follows:

TABLE I. Lennard-Jones interaction parameters.

	σ (Å)	ϵ (kcal/mol)
	H_2O[a]	
O	3.166	0.155
H	1.000	0.056
	C_2H_5OH	
C[b]	3.800	0.050
H[b]	2.500	0.050
O[b]	3.070	0.170
H(OH)[a]	1.000	0.056
	HLi	
H[c]	2.00	0.070
Li[d]	2.126452	0.018279

[a]From Ref. 2.
[b]From Ref. 27.
[c]From Ref. 28.
[d]From Ref. 29.

$$V_i = \rho \sum_{\gamma} q_\gamma C_i \left(\frac{\pi}{\alpha_i}\right)^{3/2} \int_0^\infty 4\pi r^2 \frac{\mathrm{erf}(\sqrt{\alpha_i} r)}{r} h_{\alpha\gamma}(r) dr \quad (i \in \alpha). \tag{16}$$

The exponents of the functions α_i and the number of ABSs are determined using the algorithm employed in the GAUSSIAN 03.[8,11]

RISM and these expressions have been implemented by us in GAMESS.[12] A robust solver for RISM calculation is also implemented (see Appendix). The integration of Eqs. (5) and (6) is calculated using the Obara-Saika recursions.[13,14] All calculations are performed with GAMESS (Ref. 12) and GAUSSIAN 03.[11]

IV. RESULTS AND DISCUSSION

RISM-SCF-SEDD is applied to H_2O, C_2H_5OH, and HLi in aqueous phase. The calculation in this article is performed by restricted Hartree-Fock with 6-31G* (Refs. 15 and 16) for H_2O and C_2H_5OH, and with 6-31G** (Ref. 17) for HLi.[18] The Lennard-Jones parameters are summarized in Table I. For comparison in the charge determination, two sets of grid points are prepared for the LSF procedure in the original RISM-SCF. The grid points employed in this work consist of radial part and angular part; the radial part is prepared from 5 to 50 bohrs (set A) and from 10 to 50 bohrs (set B) and angular part is based on deltoidal icositetrahedron (vertex 26).

A. H_2O

H_2O is one of the typical molecules studied by many chemists. In this section, electrostatic structure (charge and dipole moment) and solvation structure calculated by RISM-SCF-SEDD and the original RISM-SCF are presented.

The charges evaluated by RISM-SCF-SEDD ($\mathbf{q}_S$) and the original RISM-SCF calculated using the set A and set B grids ($\mathbf{q}_A$ and $\mathbf{q}_B$, respectively) are shown in Table II, where the dipole moments calculated by these methods are also shown. In the case of H_2O, there is little difference between

TABLE II. Charges and dipole moment for H_2O derived from RISM-SCF-SEDD and the original RISM-SCF with sets A and B.

	$\mathbf{q}_S$	$\mathbf{q}_A$	$\mathbf{q}_B$
O	−0.974	−0.994	−0.993
H	0.487	0.497	0.496
Dipole moment (D)	2.699	2.737	2.747

$\mathbf{q}_A$ and $\mathbf{q}_B$. Although the absolute value of $\mathbf{q}_S$ is somewhat smaller than $\mathbf{q}_{A/B}$, they are very similar to each other. The difference in the dipole moment is also very small. By comparing with the experimental value of dipole moment (2.6 D), it is shown that RISM-SCF-SEDD and the original RISM-SCF give reasonable evaluation in electrostatic structures.

RDFs calculated by RISM-SCF-SEDD and those by the original RISM-SCF are shown in Fig. 1. The sharp peak located around 1.9 Å corresponds to hydrogen bond between H and O. These methods correctly evaluate the height and the positions of these peaks.

B. C_2H_5OH

C_2H_5OH has buried sites, C_1 of CH_3 group and C_2 of CH_2 group, and the effective charges of these atoms in gas phase have been studied in detail.[19,20]

$\mathbf{q}_S$ derived from RISM-SCF-SEDD and $\mathbf{q}_{A/B}$ derived from the original RISM-SCF of C_1, C_2, and O are shown in Fig. 2. They are plotted along the RISM-SCF cycle. The charge at iteration cycle=1 corresponds to that in gas phase. $\mathbf{q}_{A/B}$ significantly depends on the choice of grid sets even in gas phase. $\mathbf{q}_B$ of C_1 is almost zero but $\mathbf{q}_A$ is negative. The difference in charges derived from the grid set becomes large as iteration cycle increases. The change of $\mathbf{q}_A$ from gas phase to aqueous phase is not so large. On the other hand, $\mathbf{q}_B$ monotonously increases or decreases and eventually diverges. Such divergence sometimes occurs in the calculation of the original RISM-SCF when the buried sites exist in a solute molecule. In the case of RISM-SCF-SEDD, the grid set is not needed and the converged $\mathbf{q}_S$ is similar to the con-

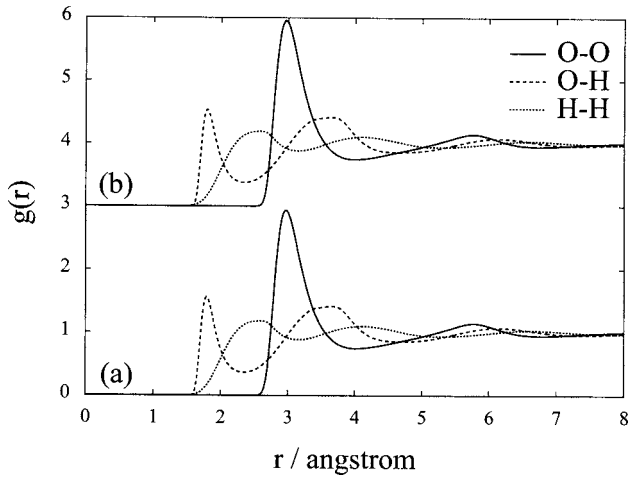

FIG. 1. RDFs of H_2O derived from (a) RISM-SCF-SEDD and (b) the original RISM-SCF.

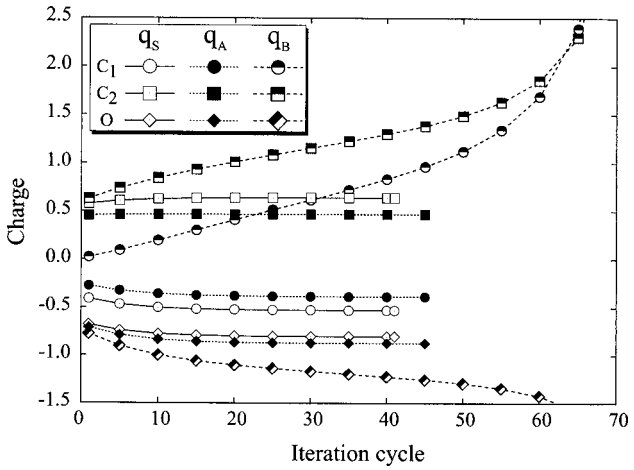

FIG. 2. The change of q_S, q_A, and q_B of C_1, C_2, and O along the RISM-SCF iteration cycle.

verged $\mathbf{q}_A$. The stability of $\mathbf{q}_S$ and the independence of grid points show that RISM-SCF-SEDD is superior to the original RISM-SCF when buried sites exist.

The RDFs calculated by RISM-SCF-SEDD and the original RISM-SCF are shown in Fig. 3. Those computed with $\mathbf{q}_S$ and with $\mathbf{q}_A$ look very similar as in the case of H_2O, while the peaks corresponding to hydrogen bonding (~2.0 Å) by RISM-SCF-SEDD are somewhat lower than those by the original one.

C. HLi

HLi is a very simple molecule but the polarization induced by solvent is very large. The natural charges[21,22] calculated with PCM (Ref. 23) ($\mathbf{q}_N$), $\mathbf{q}_S$, and $\mathbf{q}_A$ are shown in Table III. The corresponding gas values are also shown in Table III. In gas phase, the values calculated by all these methods are almost the same with each other. However, the charge deviation between H and Li in $\mathbf{q}_A$ is much stronger than that in $\mathbf{q}_S$ and $\mathbf{q}_N$ in aqueous phase.

RDFs provided by RISM-SCF-SEDD and the original RISM-SCF are shown in Figs. 4(a) and 4(b). The schematic

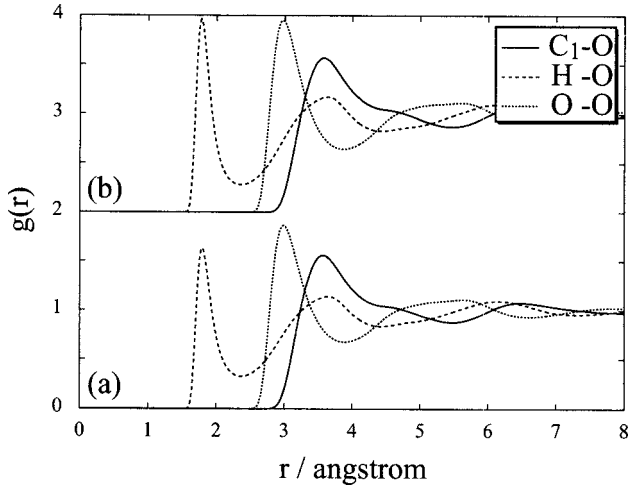

FIG. 3. RDFs of C_2H_5OH derived from (a) RISM-SCF-SEDD and (b) the original RISM-SCF.

TABLE III. Charges, $\mathbf{q}_S$, $\mathbf{q}_A$, and $\mathbf{q}_N$ for H site of HLi molecule calculated in gas phase and in aqueous phase.

	$\mathbf{q}_S$	$\mathbf{q}_A$	$\mathbf{q}_N$
H in gas phase	−0.756	−0.763	−0.730
H in aqueous phase	−1.044	−1.384	−0.887

solvation structures are shown in the right-upper side of Fig. 4(a). Sharp peaks located around 1.35 (peak a) and 2.09 Å (peak b) in Fig. 4(a) correspond to direct interactions, H–H and O–Li, respectively. They originate from the strong Coulomb interaction between H–H and O–Li. Compared to peak a and peak b, the peaks located around 2.35 (peak c) and 2.80 Å (peak d) are broad, since they correspond to indirect interaction as shown in the schematic figure. Peak d is moderately broad compared to peak c. The difference in these peaks shows that solvent H can move around a solute molecule more easily than the solvent O can. The solvation structures by the original RISM-SCF are very different from those by RISM-SCF-SEDD. For example, H–H (peak e) and Li–O RDFs, which correspond to direct interaction, are too high. In particular, peak e looks like that obtained in solid state. This is because the ESP derived from $\mathbf{q}_A$ is very strong.

In RISM-SCF procedure, ESP is expressed by point

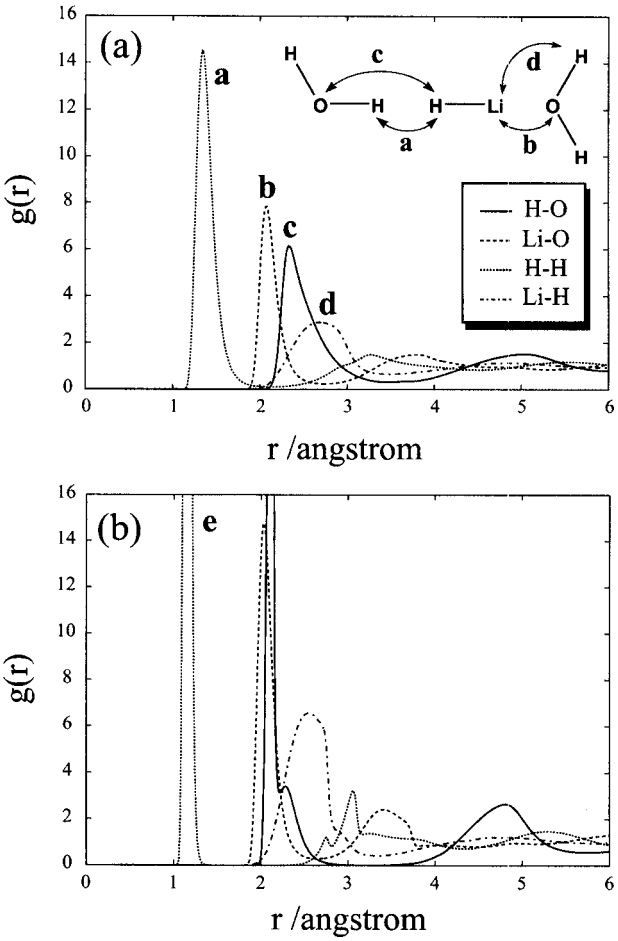

FIG. 4. RDFs of HLi derived from (a) RISM-SCF-SEDD and (b) the original RISM-SCF. Schematic figures of solvation structure around Li and around H are shown.

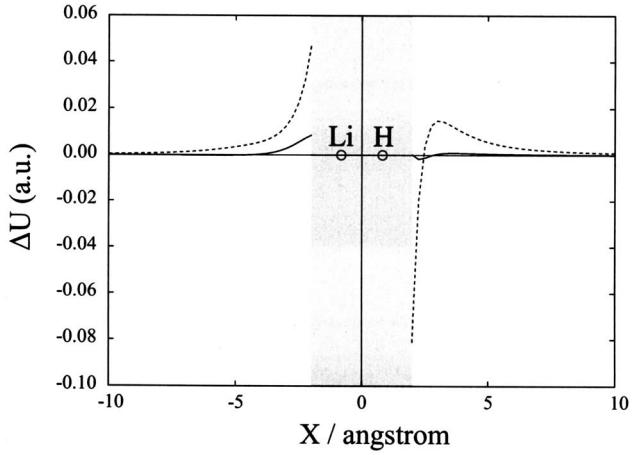

FIG. 5. The difference of the ESP evaluated by RISM-SCF-SEDD and by the original RISM-SCF from that calculated by QM calculation along HLi bond. The solid and dotted lines correspond to ΔU^{SEDD} and ΔU^{ORG}. The shaded area shows the region where the distance from solute site is shorter than the LJ parameter, $\sigma/2$.

charges or ABSs that are determined so as to reproduce the ESP directly computed from the electron density, i.e., molecular orbitals (U_{MO}). The accuracy of the fitted ESP (U_{fit}) by the point charges or ABSs can be examined by measuring the deviation from the original ESP, $\Delta U = U_{\mathrm{fit}} - U_{\mathrm{MO}}$. It should be noted that the converged electron densities of RISM-SCF-SEDD and of the original RISM-SCF are slightly different from each other. We thus defined the deviation, ΔU^{SEDD} and ΔU^{ORG}, respectively.

In Fig. 5, the ΔU^{SEDD} and ΔU^{ORG} along the H–Li bond are shown. U_{fit} reproduces U_{MO} very well in the case of RISM-SCF-SEDD. On the other hand, U_{fit} by the original RISM-SCF ($\mathbf{q}_{\mathrm{A}}$) is considerably different from the U_{MO}: ΔU^{ORG} is strongly positive, especially in the region of $X<0$ and $2.5<X<5.0$ Å, while it is negative in the region close to the solute H ($2.0<X<2.5$ Å). These discrepancies seem to be insensitive to the choice of the grid points and ΔU^{ORG} does not change so much even the grid range is shifted to the shorter distance (from 5 to 20 bohrs). This deviation in the fitted ESP is very crucial to determine the RDFs and is related to unphysical peaks in the original RISM-SCF, such as peak e depicted in Fig. 4(b).

V. CONCLUSIONS

We developed the new generation of RISM-SCF, RISM-SCF-SEDD. The main advantages of the present method are that it includes explicitly spatial distribution of electron density and that it is grid-free and robust compared to the original RISM-SCF. In this article, the independence of the grids and the origin of the stability of the calculation are discussed from the definition of the matrices used in the charge determination.

RISM-SCF-SEDD was applied to H_2O, C_2H_5OH, and HLi in aqueous phase. The charges derived from the method are very stable and reasonable both in the case of H_2O, which is typical example, and in the case of C_2H_5OH, which has buried sites. In the case of HLi, the polarization in charges between H and Li is strongly enhanced in water. With RISM-SCF-SEDD, the origin of the polarization was clearly discussed from the solvation structures, which is difficult with the original RISM-SCF.

ACKNOWLEDGMENTS

This work has been financially supported in part by the Grant-in Aid for Scientific Research on Priority Areas "Water and biomolecules" (430-18031019), "Molecular Theory for Real Systems" (461), by the Grant-in Aid for Encouragement of Young Scientists (17750012). One of the authors (D.Y.) thanks the Grant-in Aid for JSPS Fellows. The authors were supported by the Ministry of Education, Culture, Sports, Science and Technology (MEXT) Japan.

APPENDIX: A ROBUST SOLVER FOR RISM

In RISM, the iterative calculation is needed. When the interaction between solute and solvent is very large, the calculation sometimes diverge, especially at early stage of the computation. To solve RISM in stable manner, a robust solver is developed in this work.

Hypernetted-chain (HNC) closure is given by

$$h_{\alpha\beta}(r) = \exp(\chi_{\alpha\beta}(r)) - 1, \tag{A1}$$

$$\chi_{\alpha\beta}(r) = -\frac{1}{k_B T} u_{\alpha\beta}(r) + h_{\alpha\beta}(r) - c_{\alpha\beta}(r), \tag{A2}$$

where $c_{\alpha\beta}(r)$ is the direct correlation function, $h_{\alpha\beta}(r)$ is total correlation function, k_B is Boltzmann constant, and $u_{\alpha\beta}(r)$ is the pair potential between sites α and β. Equation (A1) is very unstable when $\chi_{\alpha\beta}(r)$ is large.

With a parameter F, Eq. (A1) is rearranged by

$$\begin{aligned} h_{\alpha\beta}(r) &= \exp[F + (\chi_{\alpha\beta}(r) - F)] - 1 \\ &= \exp(F)\left[\sum_{n=0} \frac{1}{n!}(\chi_{\alpha\beta}(r) - F)^n\right] - 1. \end{aligned} \tag{A3}$$

When $(\chi_{\alpha\beta}(r) - F)$ is small enough, we can truncate the expansion up to $n=1$. A new artificial "closure" is then constructed as follows:

$$h_{\alpha\beta}(r) = \begin{cases} \exp(F)[1 + (\chi_{\alpha\beta}(r) - F)] - 1 & (\chi_{\alpha\beta}(r) > F) \\ \exp(\chi_{\alpha\beta}(r)) - 1 & (\chi_{\alpha\beta}(r) \leqslant F). \end{cases} \tag{A4}$$

When $F=0$, Eq. (A4) corresponds to Kovalenko-Hirata-type closure.[24]

In general, the calculation of total correlation function, $h_{\alpha\beta}(r)$, by Kovalenko-Hirata closure is more robust than that by HNC closure. To evaluate correlation functions in stable manner especially at the beginning of the RISM iteration, F is gradually increased in a stepwise fashion. In each F value, iterative calculation between RISM and Eq. (A4) is performed until the convergence is achieved. When F becomes sufficiently large, the equation is switched from Eq. (A4) to the normal HNC closure (A1). This solver is more robust than the previous one used in our original RISM-SCF program.

[1] J. Tomasi, B. Mennucci, and R. Cammi, Chem. Rev. (Washington, D.C.) **105**, 2999 (2005).
[2] S. Ten-no, F. Hirata, and S. Kato, J. Chem. Phys. **100**, 7443 (1994).
[3] H. Sato, F. Hirata, and S. Kato, J. Chem. Phys. **105**, 1546 (1996).
[4] D. Chandler and H. C. Andersen, J. Chem. Phys. **57**, 1930 (1972).
[5] F. Hirata and P. J. Rossky, Chem. Phys. Lett. **83**, 329 (1981).
[6] *Molecular Theory of Solvation*, edited by F. Hirata (Kluwer, Dordrecht, 2003).
[7] P. M. W. Gill, B. G. Johnson, J. A. Pople, and S. W. Taylor, J. Chem. Phys. **96**, 7178 (1992).
[8] The number of ABSs (N_{ABS}) in Eq. (2) and the set of exponents $\{\alpha_i\}$ employed in Eq. (15) are systematically generated by the algorithm used in GAUSSIAN 03 (Ref. 11), which we completely followed in the present work. At first a set of exponents, $\{\alpha_i'\}$, is prepared from the set of exponents of the primitive atomic orbitals used for the MO calculation of the solute molecule ($\{\beta_i\}$) by the following equation:

$$\alpha_i' = \begin{cases} \beta_i & (i=1) \\ 2\beta_i & (i=2\cdots N_p), \end{cases}$$

where N_p is the number of the primitive atomic orbitals. The final set of $\{\alpha_i\}$ used in Eq. (15) is determined after modifying or removing the exponents that are too close to the neighboring ones. N_{ABS} is consequently determined after this modification. The N_{ABS} used in the present work was 17 for H_2O, 51 for C_2H_5OH, and 14 for HLi, respectively.
[9] This type of problems could be avoided by introducing the penalty function employed in the RESP (Ref. 20) and PDCNP (Ref. 25) procedure. However, we would like to emphasize that the obtained charges still depend on the parameters used in the penalty function. In the GJPT procedure, such function is not required.
[10] In this work, the coefficient, C_i, is determined so that $X_{ii}=1$. If the coefficient is set as $C_i=\left(\frac{\alpha_i}{\pi}\right)^{3/2}$, Z_i in Eq. (7) becomes simple to be 1.
[11] M. J. Frisch, G. W. Trucks, H. B. Schlegel *et al.*, GAUSSIAN 03, Revision C.02 Gaussina, Inc., Wallingford, CT, 2004.
[12] M. W. Schmidt, K. K. Baldridge, J. A. Boatz *et al.*, J. Comput. Chem. **14**, 1347 (1993).
[13] S. Obara and A. Saika, J. Chem. Phys. **84**, 3963 (1986).
[14] R. Ahlrichs, Phys. Chem. Chem. Phys. **8**, 3072 (2006).
[15] R. Ditchfield, W. J. Hehre, and J. A. Pople, J. Chem. Phys. **54**, 724 (1971).
[16] W. J. Hehre, R. Ditchfield, and J. A. Pople, J. Chem. Phys. **56**, 2257 (1972).
[17] P. C. Hariharan and J. A. Pople, Theor. Chim. Acta **28**, 213 (1973).
[18] The internal geometry of H_2O is 109.47° and 1 Å for the HOH angle and OH distance, respectively (Ref. 26).
[19] A. Morita and S. Kato, J. Phys. Chem. A **106**, 3909 (2002).
[20] C. I. Bayly, P. Cieplak, W. D. Cornell, and P. A. Kollman, J. Phys. Chem. **97**, 10269 (1993).
[21] J. P. Foster and F. Weinhold, J. Am. Chem. Soc. **102**, 7211 (1980).
[22] A. E. Reed, R. B. Weinstock, and F. Weinhold, J. Chem. Phys. **83**, 735 (1985).
[23] E. Cancés, B. Mennucci, and J. Tomasi, J. Chem. Phys. **107**, 3032 (1997).
[24] A. Kovalenko and F. Hirata, J. Chem. Phys. **110**, 10095 (1999).
[25] K. Ando, J. Phys. Chem. B **108**, 3940 (2004).
[26] L. X. Dang, J. E. Rice, J. Caldwell, and P. A. Kollman, J. Am. Chem. Soc. **113**, 2481 (1991).
[27] P. H. Lee and G. M. Maggiora, J. Phys. Chem. **97**, 10175 (1993).
[28] J. Gao and X. Xia, J. Am. Chem. Soc. **115**, 9667 (1993).
[29] The parameters are taken from "OPLS-AA" set developed by the W. L. Jorgensen group (Yale University), which are shown in the user manual of TINKER program package.